# The Misselhorn Cycle: Batch-evaporation process for efficient low temperature waste heat recovery

***Moritz Gleinser [a], Christoph Wieland [b] and Hartmut Spliethoff [c]***

*[a] Institute for Energy Systems, TU München, Garching, Germany, moritz.gleinser@tum.de (**CA**),*
*[b] Institute for Energy Systems, TU München, Garching, Germany, wieland@es.mw.tum.de,*
*[c] Institute for Energy Systems, TU München, Garching, Germany, spliethoff@tum.de,*
*ZAE Bayern, Bavarian Center for Applied Energy Research, Garching, Germany.*

**Abstract:**

The concept of the Misselhorn-cycle is introduced as a power cycle that aims for efficient waste heat recovery of temperature sources below 100 °C. The basic idea shows advantages over a standard Organic Rankine Cycle (ORC) in overall efficiency and utilization of the heat source. The main characteristic of this cycle is the use of at least three parallel batch evaporators instead of continuous heat exchangers. The operational phases of the evaporators are shifted so that there is always one vaporizer in discharge mode. In an isochoric batch-evaporation, the pressure and the corresponding boiling temperature rise over time. With a gradually increasing boiling temperature no pinch point limitation occurs. Furthermore, the heat source medium is passed through the evaporators in serial order to obtain a quasi-counter flow setup. These features offer the possibility to gain both high thermal efficiencies and an enhanced utilization of the heat source at the same time. A transient Matlab model is used to simulate the achievable performance of the Misselhorn Cycle. The calculations of the thermodynamic states of the system are based on the heat flux, the equations for energy conservation and the REFPROP [1] equations of state. A basic model with a fixed heat transfer coefficient promises a possible system exergy efficiency of 42.8%, which is an increase of over 50% compared to a basic ORC with a system exergy efficiency of only 27.4%. In addition to this purely thermodynamic evaluation of the process, a more detailed shell-and-tube model was developed. This advanced model includes heat transfer calculations based on the fluid flow and the shell-side liquid level. A finite differencing method is implemented to solve the partial differential equations of state and 1-D flow in the tubes. Early results of the detailed model also show a significant improvement over a common ORC.

**Keywords:**

Waste heat recovery, Low temperature, Batch evaporation, Transient simulation.

# 1. Introduction

Worldwide rising energy demands and the growing international environmental awareness cause new challenges for the energy market. As the conventional fossil fuels are more and more controversially discussed, renewable energy sources and the improvement in efficiency both gain in importance. A lot of research is already made in using renewable energy sources in geothermal, biomass, wind and solar thermal power plants. While solar and wind energy are subject to high fluctuations, the geothermal energy is continuous, but strongly depends on the temperature and quality of the water reservoir. Another environmentally sustainable approach is the conversion of surplus thermal energy from industry and power generation which is not used yet. Using waste heat from industrial processes or excess heat from gas turbines and engines to generate electrical power would improve the overall efficiency of these applications and save resources. The common basis of all these thermal energy sources is the relative low to medium temperature level they can offer. A modern steam cycle in a power plant is operated at temperatures around 600 °C [2]. Changing the working fluid to an organic medium, known as Organic Rankine Cycle (ORC), can allow temperatures down to 100 °C to be utilized, but the efficiencies are always lower in these ranges.

The major reasons for the weak performance at low temperatures are the irreversible losses in the heat exchangers due to temperature differences between the heat source and the working fluid [3]. While the liquid heat source medium is cooling down with a nearly constant slope, the evaporation of the working fluid consists of different parts. The heating of the subcooled working fluid also shows a nearly linear profile whereas the evaporation itself happens at a constant temperature. To keep a reasonable heat exchanger area, the temperature difference between the two fluids has to be bigger than a certain value, normally 5 to 10 K, at every position. Therefore the possibility to match the two temperatures is limited by the occurring pinch point as shown in Fig. 1(a).

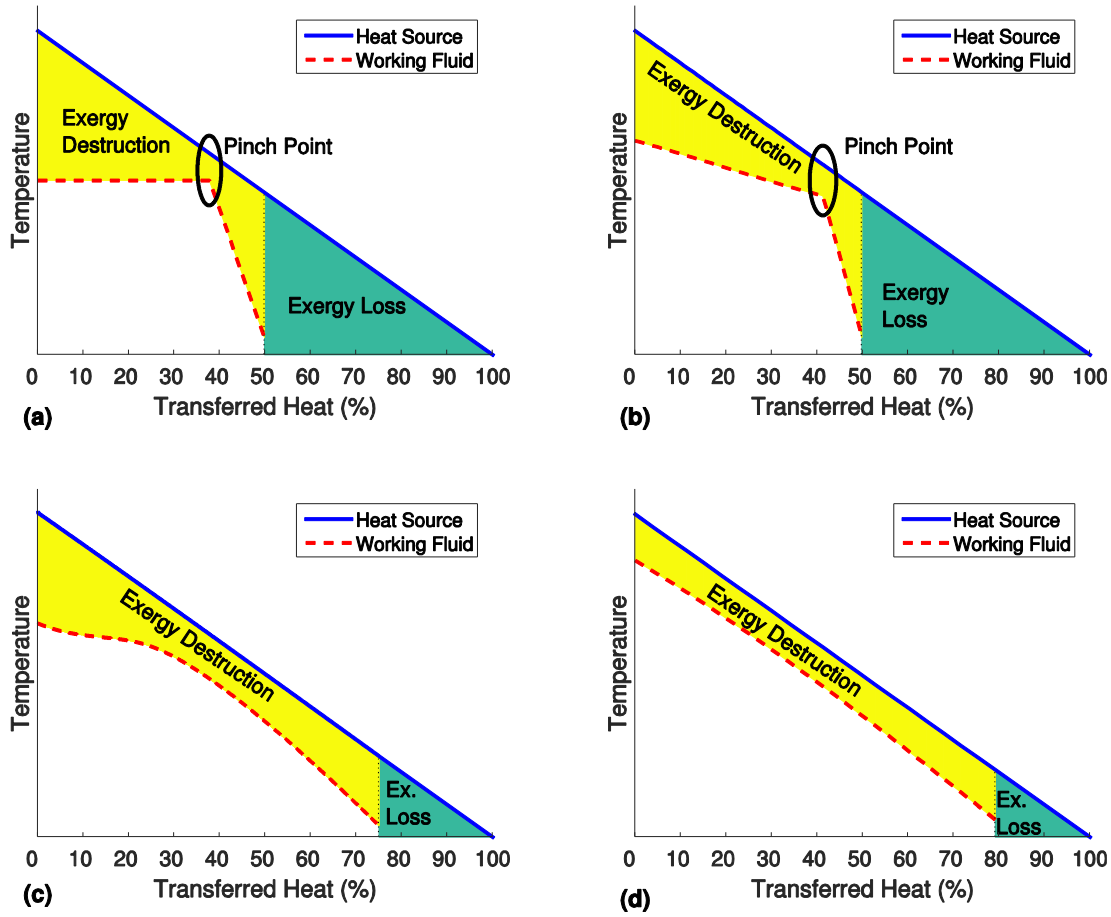


*Fig. 1. Qualitative comparison of the temperature match in different power cycles: a) common ORC, b) zeotropic cycle, c) supercritical cycle, d) flash cycle.*

The best method to rate the efficiency of a process depends strongly on the given application. In this context an often used property is the exergy $Ex$. It describes the maximum work that can theoretically be created from a heat source with respect to a given dead state. For a common power cycle with a closed heating circuit, the most important parameter is the efficiency of converting the heat that is actually added. This depends on the available vapour pressure, the efficiency of the turbine and on the heat transfer itself. If heat is transferred from a high grade heat source to a lower temperature working fluid exergy is destroyed (see Fig. 1 (a)). In contrast, many waste heat recovery applications have an open heating circuit where any unused heat is discarded and lost. This unused exergy accounts as exergy loss. Therefore, the goal is to achieve a combination of a high utilization of the heat source, a good temperature match and an acceptable conversion efficiency.

There are several concepts to reduce the exergy destruction and losses. As shown in Fig. 1 (b) the boiling temperature of a mixture of different fluids will rise during the evaporation [4] as the low boiling component will vaporize first and the high boiling part will accumulate in the residue.

Another method is the operation close to critical conditions. Especially in supercritical cycles, there is no distinction between fluid and vapour phases. Without the temperature plateau during phase

change the temperature match can be improved [5] as shown in Fig. 1 (c). A disadvantage of this process is the challenging design of the turbine that has to deal with a supercritical working fluid.

Flash cycles focus on single-phase liquid-liquid heat exchange to avoid the pinch point limitation completely. With suitable mass flows, the temperature difference can be equally small over the entire heat exchanger (Fig. 1 (d)). The power generation can then either be performed in a two-phase expander [6] or, as in the Organic Flash Cycle [7], the saturated liquid is flash evaporated and the vapour is expanded in a common turbine. While the former one is still depending on the ongoing two-phase exchanger research, the latter one has to deal with major exergy losses in the throttling valve or in alternative with a more complex process setup [8].

The thermodynamic fundamentals of the Misselhorn Cycle were first introduce in [9]. A more viable process setup, as suggested in [10], already combines two of the main objectives of the current state of the cycle. The working fluid is vaporized in a closed batch evaporation. Due to the isochoric phase change, the saturation temperature rises with the ongoing process, the constant temperature phase can be avoided and a closer match to the heat source temperature can be achieved. In addition, the pressure is completely generated by the isochoric evaporation. Therefore the power consumption of the feed pump can be considerably reduced. In this paper, an additional cascaded dynamic heat source flow through several heat exchangers in series is introduced. This setup ensures the ideal assignment of temperature levels of the heat source to the corresponding evaporation phases. Transient Matlab simulations are conducted to analyse the thermodynamic possibilities of this power cycle and compare it to a common ORC.

# 2. Description and analysis of the Misselhorn Cycle

## 2.1. Basic concept of the Misselhorn Cycle

The basic setup of the Misselhorn Cycle as shown in Fig. 2 is similar to a common ORC. A liquid organic working fluid is evaporated in a heat exchanger, expanded in an expansion engine and condensed in another heat exchanger. The major difference is the non-continuous mode of operation and the pressure levels.

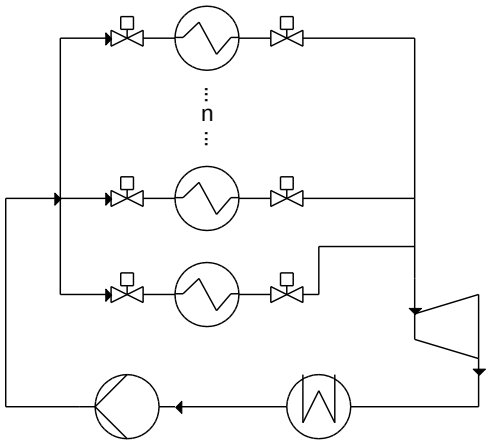


*Fig. 2. Process flow diagram of the basic Misselhorn Cycle.*

In a first phase, the working fluid is pumped into a heat exchanger at condenser pressure. In the second phase, the evaporator inlet and outlet valves are both closed and the working fluid is at least partly vaporized. Due to the isochoric process, both the pressure and the corresponding boiling temperature of the working fluid rise. Once a certain pressure is reached, the outlet valve is opened and the vapour flows into the expansion engine (phase three). After a defined time, the operating phases are switched again and the now almost empty vaporizer is refilled. To provide a continuous steam flow, at least three parallel heat exchangers are needed. They are run with shifted phases so that there is always one evaporator in the discharging phase. Regarding the fluctuating vapour outlet

parameters a modified diesel engine is chosen over a turbine as expansion engine. In this basic setup [10], the heat source flow is split and runs through all heat exchangers in parallel.

## 2.2. Methods of analysis

As basis for the further analysis and discussions the following efficiencies are useful.

The most commonly used efficiency to characterize a power cycle is the **thermal efficiency**

$$\eta_{\text{therm}} = \frac{P_{\text{output}}}{\dot{Q}_{\text{in}}}. \qquad (1)$$

It is defined by the ratio of the power output of the expansion engine $P_{\text{output}}$ versus the actually added heat flow to the cycle $\dot{Q}_{\text{in}}$. This contains no information about the utilization of the heat source but only about the performance of the cycle itself. If heat that is not transferred will still be used in further processes or cogeneration this efficiency can be useful.

In practice, the maximum work that can be gained from a given heat source with respect to the limitations of the second law of thermodynamics is called the exergy. The specific exergy is generally defined as

$$ex = (h - h_0) - T_0 \cdot (s - s_0), \qquad (2)$$

where $h$ and $s$ are enthalpy and entropy at the current state and the index $0$ denotes the values at a reference point. The reference state $T_0$ is normally set to the ambient conditions or the temperature of the heat sink. Following this definition, the exergy of a stream will be zero at the reference state.

The heat flow in (1) can be replaced by the exergy flow that is released from the heat source in the evaporator. This exergy flow $\dot{E}x_{\text{in}} = \dot{m}_{\text{hs}} \cdot (ex_{\text{hs,in}} - ex_{\text{hs,out}})$ can be calculated from the heat source mass flow $\dot{m}_{\text{hs}}$ and the drop of the specific exergy over the heat exchanger. The **thermal exergy efficiency** then follows as

$$\eta_{\text{therm, EX}} = \frac{P_{\text{output}}}{\dot{E}x_{\text{in}}}. \qquad (3)$$

Note that the exergy destruction during heat transfer is included here as the exergy added to the working fluid is less than the exergy released from the heat source ( $\dot{E}x_{\text{in}}$ ) due to irreversibility.

To additionally account for the needed auxiliary power, the **net efficiency** can be used:

$$\eta_{\text{net}} = \frac{P_{\text{output}} - P_{\text{auxilliary}}}{\dot{Q}_{\text{in}}} = \frac{P_{\text{net}}}{\dot{Q}_{\text{in}}}. \qquad (4)$$

Here the gross power output is reduced by the demand of additional components such as the feed pump and the supply pumps for the heat source medium and the cooling medium. This is also often referred to as first law efficiency. As for the thermal efficiency (1), the heat flow can be replaced by the exergy flow to get the **net exergy efficiency** (also called external second law efficiency)

$$\eta_{\text{net, EX}} = \frac{P_{\text{net}}}{\dot{E}x_{\text{in}}}. \qquad (5)$$

To rate the utilization of the heat source the **heat exchanger efficiency** can be introduced as

$$\eta_{\text{HX}} = \frac{\dot{m}_{\text{hs}} \cdot (ex_{\text{hs,in}} - ex_{\text{hs,out}})}{\dot{m}_{hs} \cdot \left( ex_{\text{hs,in}} - \underbrace{ex_{\text{hs,0}}}_{=0} \right)} = \frac{\dot{E}x_{\text{in}}}{\dot{E}x_{\text{av}}}. \qquad (6)$$

This efficiency is based on the ratio of the exergy that is released from the heat source versus the maximum exergy that is available from the heat source. Any lost exergy is accounted by this rating.

As overall characteristic the **system efficiency** is defined as

$$\eta_{\mathrm{sys,EX}} = \eta_{\mathrm{HX}} \cdot \eta_{\mathrm{net,EX}} = \frac{\dot{E}x_{\mathrm{in}}}{\dot{E}x_{\mathrm{av}}} \cdot \frac{P_{\mathrm{net}}}{\dot{E}x_{\mathrm{in}}} = \frac{P_{\mathrm{net}}}{\dot{E}x_{\mathrm{av}}}. \quad (7)$$

An efficient system is dependent on both a good heat transfer ability (6) and an efficient heat-to-power conversion (5). As combination of these two factors, the system efficiency represents the net power that can be created from a given finite heat source.

The heat exchanger and system efficiency can also be defined based on the heat transfer instead of the exergy flow, but in this work only the two introduced ones will be used.

## 2.3. Advantages of the Misselhorn Cycle

In the Misselhorn Cycle heat is transferred from one continuously flowing heat source to the pool of working fluid in the heat exchangers. The closed batch evaporation can best be shown in a piecewise T-Q-diagram of one heat exchanger as presented in Fig. 3 (a). For illustrative reasons the evaporation sequence is divided into several theoretical time steps of the same length. The actual calculations of the process are performed with a finer resolution. Beginning with the lowest temperature of the working fluid on the right side, heat is transferred from the heat source medium to the working fluid. The pressure and the boiling temperature of the working fluid are assumed constant during one time step while the heat source is cooled down. In any following time steps the pressure and the corresponding boiling temperature of the working fluid are higher due to the isochoric process. As this is not a counter flow setup but a sort of pool boiling, the working fluid is in exchange with fresh and hot heat source medium in every time step. The rising temperature of the working fluid causes a decreasing temperature difference and therefore the transferred heat in each time step becomes smaller (the width of the steps decreases). Accordingly the cooling of the heat source is reduced. As a result of the continuously rising boiling temperature there is no distinct pinch point until the end of the evaporation.

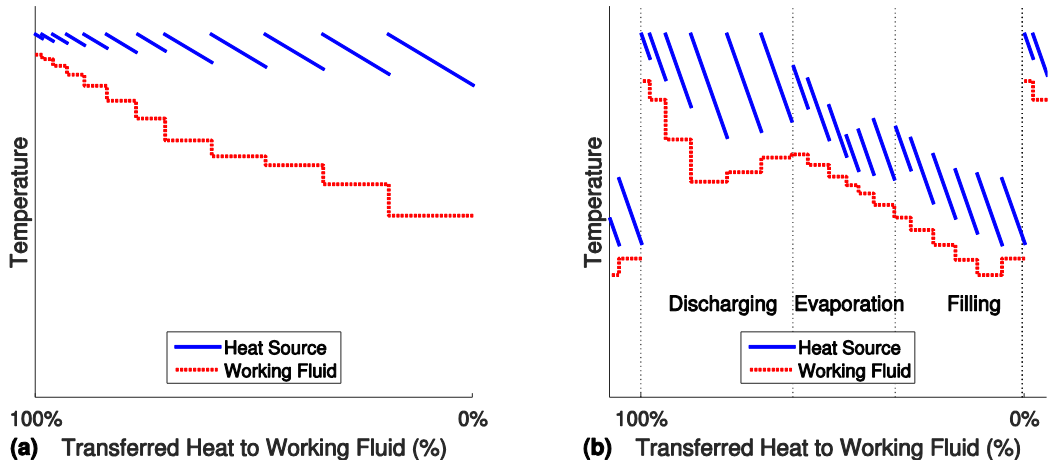


*Fig. 3. Qualitative piecewise T-Q-diagrams of the basic ideas of the Misselhorn Cycle: a) Batch evaporation, b) Cascading heat source circuit.*

It can be seen from Fig. 3 (a) that in the zone of hot working fluid, the outlet temperature of the heat source is still very high. Simultaneously, the cold working fluid does not completely use the potential of the hot heat source. Therefore the heat source flow is changed, so that it is not split, but rather flows through all heat exchanges in series. The fresh heat source medium is fed to the evaporator that is currently in the most important discharge phase (see Fig. 3 (b)). The outlet of every time step from this heat exchanger is then directed to the evaporation phase in the second heat exchanger and further to the third one. Although the outlet stream is gradually cooled down, its

temperature is still high enough to preheat the inflowing cold working fluid. Once the operating phases are switched, the heat source flow has to be adjusted accordingly. The three cycle phases in Fig. 3 (b) can be seen as the simultaneous process in three different evaporators. The six steps in each phase then correspond to the steps in the other phases. As all the heat exchangers are only shifted in time but are similar apart from that, the whole red curve also matches a complete cycle in one single evaporator over time.

Since all three phases are heated, the pressure is already building up significantly in the filling phase. In order to preserve the advantage of the low power demand for the compression, the duration ratio of evaporation versus filling is adjusted. By adding three more evaporators, the cycle phases are now: filling, evaporation phases one to four and discharge. In Fig. 4, the temperature profile of a setup with six heat exchangers is shown. By decreasing the size of the displayed time steps, the graph flattens. Also the cascading heat source curves can be replaced by one constant line if the number of evaporators is sufficient. The resulting T-Q-diagram shows a quasi-stationary and quasi-counter-flow process without any typical pinch point.

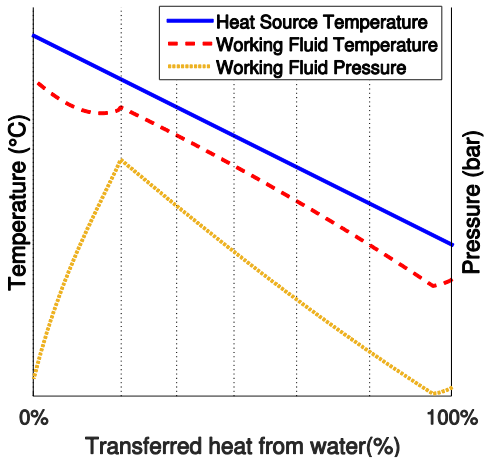


*Fig. 4. Quasi-continuous T-Q-diagram of the Misselhorn Cycle for six heat exchangers.*

The six phases of the cycle are marked by the thin dotted lines. Like in Fig. 3 (b) the one to the right is the filling and the one to left is the discharging. Due to the pressure drop during the discharge the temperature of the working fluid undergoes a short drop before the remaining mass is small enough to be heated up again quickly.

# 3. Simulation models

To evaluate the potential of the Misselhorn Cycle transient simulations are conducted in Matlab. For comparison a common ORC is modelled in Aspen Plus V8.6.

## 3.1. Aspen model of the benchmark ORC

The benchmark cycle is a common Organic Rankine Cycle without recuperator. Starting point is the heat source with a fixed temperature and mass flow. The mass flow of the working fluid is adjusted to ensure the minimum pinch point in between the preheater and the evaporator. The sizes of the heat exchangers are adjusted automatically to fulfil the required heat transfer. The outlet pressure of the turbine is chosen to fit the available heat sink temperature with respect to the necessary pinch point in the condenser. Two auxiliary pumps are added to overcome the pressure drop in the preheater, the evaporator and the condenser. All pumps and the turbine are set up with constant isentropic efficiencies.

The outlet pressure of the feed pump is the only degree of freedom of the resulting model. It is varied in the context of a sensitivity analysis to find the best efficiencies.

## 3.2. Matlab model of the Misselhorn Cycle

Given the unsteady character of the Misselhorn Cycle, a transient Matlab model is developed. The cores of the model are the mass and energy balances of the evaporator shell side

$$\frac{dm_{\mathrm{wf,HX}}}{dt} = \dot{m}_{\mathrm{wf,\,in}} - \dot{m}_{\mathrm{wf,\,out}}, \qquad (8)$$

$$\frac{dU_{\mathrm{HX}}}{dt} = \dot{H}_{\mathrm{wf,\,in}} - \dot{H}_{\mathrm{wf,\,out}} + \dot{Q}. \qquad (9)$$

To solve the changes of the mass of the working fluid $m_{wf,HX}$ and of the internal energy $U_{\mathrm{HX}}$ in one evaporator, the mass flows ($\dot{m}_{\mathrm{wf,\,in}}$ and $\dot{m}_{wf,\,\mathrm{out}}$), the enthalpy flows ($\dot{H}_{\mathrm{wf,\,in}}$ and $\dot{H}_{\mathrm{wf,\,out}}$) and the heat flow $\dot{Q}$ that is transferred from the heat source are needed. All thermodynamic states are calculated with the REFPROP database by NIST [1]. For the basic simulation, the tubes are not modelled in detail. Instead, the heat transfer factor $k \cdot A$ is assumed as constant and can be set in the context of parameter variations. From the known inlet temperature of the heat source and the temperature of the working fluid the transferred heat can be estimated using a stationary NTU approach [11] (Number of Transfer Units) for every time step. The nondimensional heat transfer ability

$$NTU = \frac{k \cdot A}{\dot{C}_{\mathrm{hs}}}, \qquad (10)$$

can be calculated from the heat transfer coefficient $k$, the heat transfer area $A$ and the heat capacity flow of the heat source $\dot{C}_{\mathrm{hs}} = \dot{m}_{\mathrm{hs}} \cdot c_{\mathrm{p,hs}}$.

As the working fluid has a constant temperature over one time step, the heat exchanger efficiency $\varepsilon$ is defined as

$$\varepsilon = 1 - \exp(-NTU). \qquad (11)$$

The actually transferred heat can then be obtained from the efficiency (11) and the maximum possible heat transfer $\dot{Q}_{\mathrm{max}}$ as

$$\dot{Q} = \varepsilon \cdot \dot{Q}_{\mathrm{max}} = \varepsilon \cdot \dot{C}_{\mathrm{hs}} \cdot \left(T_{\mathrm{hs,in}} - T_{\mathrm{wf}}\right). \qquad (12)$$

While this shortcut is adequate for a general thermodynamic evaluation of the Misselhorn Cycle, some expansions are needed in order to account for the dwell time of the heat source medium in the tubes and for the flow dependent heat transfer coefficients. By adding a basic tube geometry the flow characteristics of the heat source medium can be calculated. From the energy balance over an infinitesimal tube element the differential equations of the tube flow can be established. Assuming a 1D flow only the enthalpy flow and the heat transfer are needed for the balance of the tube elements. The resulting partial differential equation is discretised into cells and solved by a finite differencing method. Based on the characteristic numbers of the tube flow, the heat transfer is computed for every time step and every tube cell. Several correlations are included according to their range of validity for tube side heat transfer [12–16] and shell side boiling [17–19].

# 4. Results and Discussion

## 4.1. Reference Conditions

Both the simulations of the ORC and the Misselhorn Cycle are based on the same reference conditions. The heat source and heat sink conditions are summarized in Table 1. Heat is available from hot water at the temperature of 85 °C with a fixed mass flow of 6.97 kg/s. Cold water at 20 °C is used in the condenser. The reference point for exergy calculations is set to 20 °C and 1 bar. The total available exergy with these parameters is $\dot{E}x_{\mathrm{av}}$ = 184.6 kW.

*Table 1. Reference conditions for the heat source and heat sink*

| | Heat source (water) | Heat sink (water) | Reference conditions |
|---|---|---|---|
| Massflow | 6.97 kg/s | Calculated from condenser pinch point | - |
| Temperature | 85 °C | 20 °C | 20 °C |
| Pressure | 2.36 bar | 2.60 bar | 1 bar |

The component and cycle parameters are summarized in Tab. 2. As the main objective of the simulation of the Misselhorn Cycle is the heat transfer, the power generation is simplified and calculated by the isentropic expansion of the produced vapour. To estimate the needed heat exchange area the heat transfer coefficients are assumed with 1.5 kW/(m²·K) for liquid to liquid heat transfer and with 3 kW/(m²·K) for liquid to boiling. R134a is used as working fluid, to be in agreement with the test system that is currently built by the Maschinenwerk Misselhorn MWM GmbH.

*Table 2. Reference parameters of the cycle components*

| | | | |
|---|---|---|---|
| Isentropic pump efficiency | 90% | Working fluid | R134a |
| Isentropic turbine / engine efficiency | 85% | ORC pinch point | 5 K |
| Tube side pressure drop | 0.3 bar | Single phase heat transfer | 1.5 kW/(m² K) |
| Shell side pressure drop | 0.2 bar | Boiling heat transfer | 3.0 kW/(m² K) |

## 4.2. Performance of the basic ORC

The optimization of the basic ORC can be conducted by a simple sensitivity analysis over the vaporization pressure. In Fig. 5 (a) the influence of the vapour pressure on the ORC efficiencies is shown. It can be seen that the thermal / net exergy efficiencies and the heat exchanger efficiency are competing parameters. In terms of the main objective, an optimization of the system efficiency, this demands for a compromise of these values.

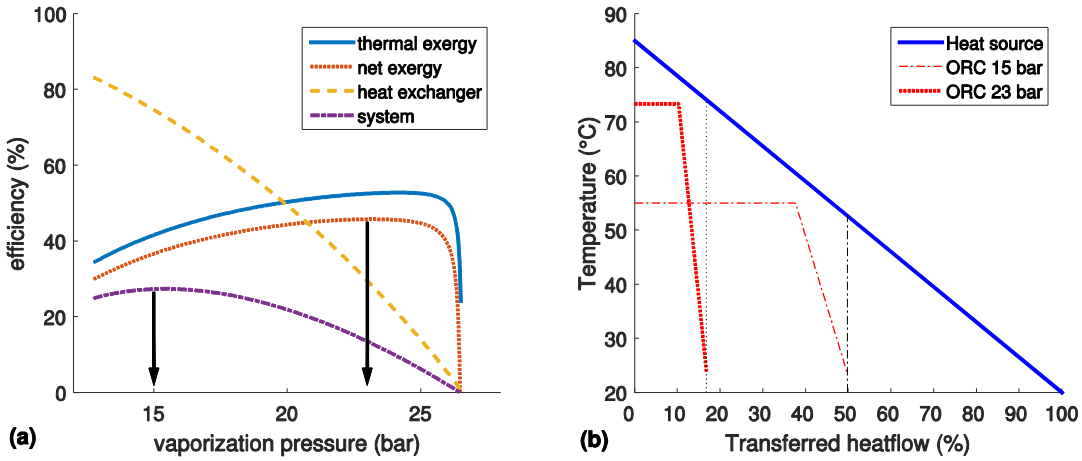


*Fig. 5. Performance of an ORC with the given heat source: a) influence of the vapour pressure on the efficiency, b) T-Q-diagram of two characteristic operating points.*

The best net exergy efficiency is reached at about 23 bar. As the heat exchanger efficiency has no maximum in the investigated range, the best system efficiency at 15 bar is chosen as a second characteristic working point of this ORC. For further discussion, the T-Q-diagram of these two characteristic operating states is shown in Fig. 5 (b).

The high pressure case shows a good temperature match with the heat source and reaches a high outlet temperature and pressure. As expected a good net exergy efficiency of 45.8% can be gained. However, with the given pinch point the heat exchanger efficiency is only 29.5% and therefore the overall power output (28.6 kW) as well as the system efficiency (13.5%) are low. A higher pressure would further increase the thermal exergy efficiency, but the transferred heat would become so small that the produced power could not even compensate the auxiliary power consumption.

In contrast, the lower pressure case can take advantage of the heat source much better which is shown by a heat exchanger efficiency of 74.6%. The disadvantage is the comparably low net exergy efficiency of only 36.6%. Still, the overall system efficiency is at a global maximum of 27.4% and the generated power of the turbine is 57.3 kW for this low pressure case. A lower pressure would allow an even better heat exchanger efficiency, but would not produce enough power in the turbine.

## 4.3. Performance of the Misselhorn Cycle

As a result of the transient character of the Misselhorn Cycle, there are many degrees of freedom that affect the performance. Due to the extensive simulation duration, a simple parameter variation was not productive. Instead, a genetic algorithm is used to optimize the target efficiency.

The possible efficiency depends strongly on the number of used heat exchangers and their heat transfer ability. In addition to the setup with six heat exchangers (see Fig. 4), the basic setup with only three evaporators and an expanded setup with ten heat exchangers are shown in Fig. 6 (a) and Fig. 6 (b) respectively.

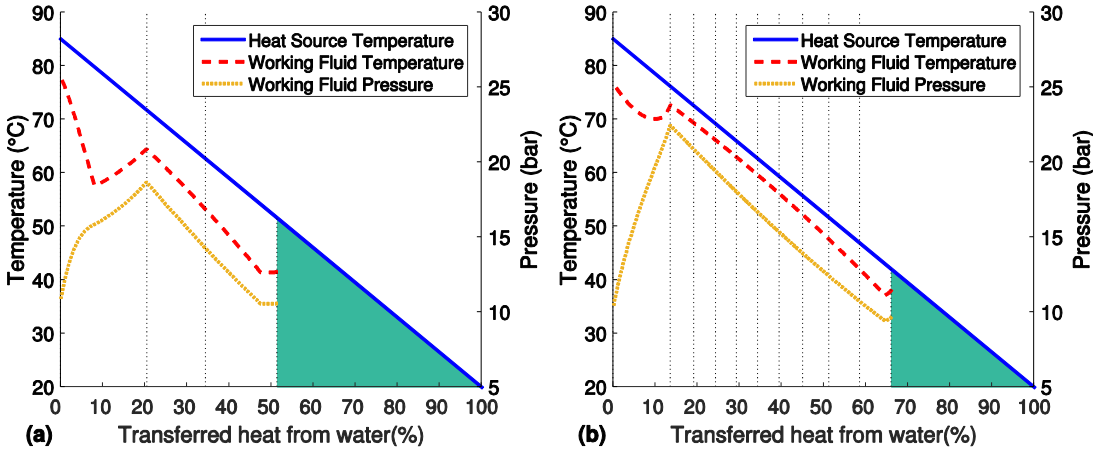


*Fig. 6. Quasi-continuous T-Q-diagrams of the Misselhorn Cycle: a) three heat exchangers, b) ten heat exchangers.*

It can be seen that more heat exchangers allow a better temperature match and a higher maximum pressure. Consequently the system efficiency can be raised from 30.9% with three heat exchangers up to 42.8% with ten heat exchangers. This improvement is based on an increasing net exergy efficiency (less exergy destruction) as well as a rising heat exchanger efficiency (less exergy losses).

## 4.4. Comparison of the Misselhorn Cycle and a common Organic Rankine Cycle

The results of the Misselhorn Cycle simulations in Table 3 show a serious advantage over a common ORC. Already the smallest setup with three heat exchangers shows an improvement of the system efficiency of more than 10 % (ORC 27.4% / MWM 30.9% / +12.8%). Although they both transfer about the same amount of heat and exergy (Ex. 138 kW, heat ~980 kW), the Misselhorn Cycle offers better thermal and net efficiencies and therefore outperforms the ORC in the power output (57 kW / 62 kW / +8.8%). In addition the power needed of the feed pump is reduced.

Moreover, the single phase heat transfer in the preheater of the ORC requires a significant fraction of the overall heat transfer area of the low pressure ORC case. As the Misselhorn Cycle takes only place in the two-phase region, the good heat transfer during boiling keeps the required transfer area of the additional heat exchangers to an acceptable value (29 m² / 35 m² / +20.7%).

Simply increasing the exchanger area of the ORC and setting a smaller pinch point would allow for a small increase in the performance. However, there is no possibility to overcome the pinch point completely. In contrast, adding more heat exchangers to the Misselhorn Cycle will significantly

increase the performance. By using six evaporators, both the net exergy efficiency and the heat exchanger efficiency can be enhanced. Thus, the system efficiency can be improved by almost 40 % compared to the ORC (27.4% / 38.2% / +39.4%). The setup with ten heat exchangers can even top these numbers with a system efficiency of 42.8 % (27.4% / 42.8% / +56.2%). Of course for this dimension the required heat exchanger area is bigger than for the ORC (29 m² / 117 m²).

*Table 3. Results for the ORC and Misselhorn Cycle*

| | ORC | | MWM | | |
|---|---|---|---|---|---|
| | 15 bar | 23 bar | 3 HX | 6 HX | 10HX |
| $P_{output}$ | 57.3 kW | 28.6 kW | 62.0 kW | 76.6 kW | 86.2 kW |
| $\dot{Q}_{in}$ | 972 kW | 318 kW | 985 kW | 1104 kW | 1260 kW |
| $\dot{E}x_{in}$ | 138 kW | 54 kW | 138 kW | 149 kW | 161 kW |
| $P_{pump}$ (feed / aux.) | 3.6 / 3.2 kW | 2.3 / 1.3 kW | 1.6 / 3.4 kW | 1.6 / 4.3 kW | 1.5 / 5.7 kW |
| $\eta_{therm,EX}$ | 41.6% | 52.6% | 45.1% | 51.5% | 53.6% |
| $\eta_{net,EX}$ | 36.6% | 45.8% | 41.5% | 47.5% | 49.2% |
| $\eta_{HX}$ | 74.6% | 29.5% | 74.5% | 80.5% | 87.1% |
| $\eta_{sys,EX}$ | 27.4% | 13.5% | 30.9% | 38.2% | 42.8% |
| overall area | 29.2 m² | 12.7 m² | 35.0 m² | 70.0 m² | 116.7 m² |
| $T_{hs,out}$ | 51.7 °C | 74.1 °C | 51.5 °C | 47.4 °C | 42.0 °C |

## 4.5. Outlook

While the basic simulation of the Misselhorn Cycle primarily evaluates the thermodynamic potential, the detailed model should represent a more practical approach. The transient nature of the process causes complex periodic temperature changes in several components such as the hot water in the heat exchanger tubes. This opens another level of temperature match that has to be accomplished. Furthermore, the actual heat transfer is not only depended on the alternating flow characteristics, but also the wetted heat transfer area changes when working fluid evaporates.

The early generations of the ongoing genetic optimization of the detailed model also show an improvement over the ORC. The current best case for a setup with six heat exchangers reaches an increase of the system efficiency of 12.7% over the ORC. It is expected to further rise in later generations. Especially the current tube geometry seems to limit the heat transfer.

The model validation will be performed based on data from the test cycle that is built at the moment by MWM. It is shown that the selection of the working fluid can highly affect the cycle performance [5, 20, 21]. Therefore it is also planned to analyse the behaviour of the Misselhorn Cycle with different fluids.

In order to evaluate the efficiency advantages in consideration of the substantial complexity of the Misselhorn Cycle an extensive economic analysis is needed.

# 5. Conclusion

The concept of the Misselhorn Cycle was introduced with its two main characteristics: batch evaporation and a dynamic cascaded heat source circuit. This results in a good temperature match of heat source and working fluid and allows for a good utilization of the available heat source at the same time (see Fig. 7). Different efficiencies were defined in order to evaluate the performance of the Misselhorn Cycle and compare it to a common ORC. In this context the exergy was used to illustrate the appearance of losses. Based on reference conditions simulations of both a benchmark ORC and the Misselhorn Cycle were performed. Depending on the number of used heat exchangers, the basic Misselhorn model showed an increase in the system efficiency (e.g. 10 evaporators, 43%) of up to 50% over the ORC (27%). Deviations from this basic thermodynamic analysis should be covered by a detailed model. The current best case of the still ongoing detailed optimization shows

an advantage in the system efficiency of 12.7%. An increase up to the 50% advantage of the basic model is expected for a further optimized operating point and with an adjusted tube geometry. The model validation is planned based on measured data from a currently built test cycle. It is further planned to analyse the applicability of different working fluids.

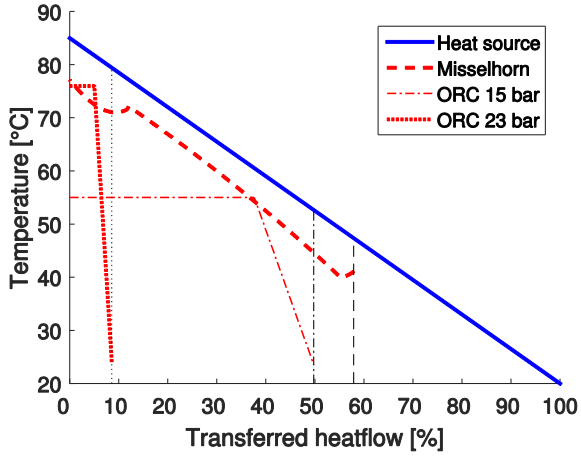


*Fig. 7. Comparison of two operating points of an ORC with the Misselhorn Cycle (setup with six heat exchangers).*

## Acknowledgments

This work was performed and funded in context of a research project with Maschinenwerk Misselhorn MWM GmbH. The MWM project is sponsored by the Bavarian Ministry of Economic Affairs and Media, Energy and Technology in context of the BayINVENT program. Special thanks go to Manfred Moullion, MWM, for the close cooperation and the detailed information about the test cycle.

## Nomenclature

| | | | |
|---|---|---|---|
| $A$ | area, m² | $\dot{m}$ | mass flow rate, kg/s |
| $c_p$ | specific heat, kJ/(kg K) | $NTU$ | number of transfer units, - |
| $\dot{C}$ | heat capacity flow rate, kJ/(s K) | $P$ | power, kW |
| $ex$ | specific exergy, kJ/kg | $\dot{Q}$ | heat flow rate, kW |
| $\dot{E}x$ | exergy flow rate, kW | $s$ | entropy, kJ/(kg K) |
| $h$ | enthalpy, kJ/(kg K) | $t$ | time, s |
| $\dot{H}$ | enthalpy flow rate, kW | $T$ | temperature, °C |
| $k$ | heat transfer coefficient, kW/(m² K) | $U$ | internal energy, kJ |

**Subscripts and superscripts**

| | | | |
|---|---|---|---|
| 0 | reference conditions | in | input |
| av | available | out | output |
| EX | exergy | therm | thermal |
| hs | heat source | wf | working fluid |
| HX | heat exchanger | | |

**Greek symbols**

| | | | |
|---|---|---|---|
| $\varepsilon$ | heat exchanger efficiency (NTU concept) | $\eta$ | efficiency |

# References


[1] Lemmon E. W., Huber M. L., McLinden M.: NIST Standard Reference Database 23: Reference Fluid Thermodynamic and Transport Properties-REFPROP, Version 7.0. Gaithersburg: National Institute of Standards and Technology, Standard Reference Data Program; 2002.

[2] Spliethoff H.: Power generation from solid fuels. Heidelberg, New York: Springer; 2010.

[3] Mago P. J., Srinivasan K. K., Chamra L. M., Somayaji C.: An examination of exergy destruction in organic Rankine cycles. Int. J. Energy Res. 2008;32(10):926-38.

[4] Heberle F., Preißinger M., Brüggemann D.: Zeotropic mixtures as working fluids in Organic Rankine Cycles for low-enthalpy geothermal resources. Renewable Energy 2012;37(1):364-70.

[5] Schuster A., Karellas S., Aumann R.: Efficiency optimization potential in supercritical Organic Rankine Cycles. Energy 2010;35(2):1033–39.

[6] Lai N. A., Fischer J.: Efficiencies of power flash cycles. Energy 2012;44(1):1017-27.

[7] Ho T., Mao S. S., Greif R.: Comparison of the Organic Flash Cycle (OFC) to other advanced vapor cycles for intermediate and high temperature waste heat reclamation and solar thermal energy. Energy 2012;42(1):213-23.

[8] Ho T., Mao S. S., Greif R.: Increased power production through enhancements to the Organic Flash Cycle (OFC). Energy 2012;45(1):686-95.

[9] Misselhorn J. (inventor); Maschinenwerke Misselhorn GmbH, 80336 München, DE: Wärmekraftmaschine. DE 10 2008 023 793 A1. 2008 May 15.

[10] Moullion M. (inventor); Maschinenwerk Misselhorn GmbH - MWM: Anlage und Verfahren zur Rückgewinnung von Energie aus Wärme in einem thermodynamischen Kreisprozess. DE 10 2013 009 351 B3. 2013 Jun 4.

[11] Polifke W., Kopitz J.: Wärmeübertragung: Grundlagen, analytische und numerische Methoden; [mit Software Scilab]. München, Boston [u.a.]: Pearson Studium; 2005.

[12] Bhatti M. S., Shah R. K.: Turbulent and Transition Flow Convective Heat Transfer in Ducts. In: Kakaç S, Shah RK, Aung W, editors. Handbook of single-phase convective heat transfer. New York: Wiley. 1987. Chapter 4.

[13] Gnielinski V.: Neue Gleichungen für den Wärme- und Stoffübergang in turbulent durchströmten Rohren und Kanälen. Forschung im Ingenieurwesen 1975;41(1):8-16.

[14] Gnielinski V.: Ein neues Berechnungsverfahren für die Wärmeübertragung im Übergangsbereich zwischen laminarer und turbulenter Rohrströmung. Forschung im Ingenieurwesen 1995;61(9):240-48.

[15] Shah R. K., London A. L.: Laminar flow forced convection in ducts: A source book for compact heat exchanger analytical data. New York: Academic Press; 1978.

[16] Shah R. K., Mueller A. C.: Heat Exchange. In: Ullmann's encyclopedia of industrial chemistry. 6th ed. Weinheim, Germany: Wiley-VCH. 2003. p. 309-419.

[17] Baehr H. D., Stephan K.: Wärme- und Stoffübertragung. Berlin, Heidelberg: Springer; 2010.

[18] Smith R. A.: Vaporisers: Selection, design & operation. Harlow, Essex, England, New York: Longman Scientific & Technical; Wiley; 1986.

[19] Webb R. L., Chien L.-H.: Correlation of Convective Vaporization on Banks of Plain Tubes Using Refrigerants 1994.

[20] Chen H., Goswami D. Y., Stefanakos E. K.: A review of thermodynamic cycles and working fluids for the conversion of low-grade heat. Renewable and Sustainable Energy Reviews 2010;14(9):3059-67.

[21] Chys M., van den Broek, M., Vanslambrouck B., Paepe M. de: Potential of zeotropic mixtures as working fluids in organic Rankine cycles. Energy 2012;44(1):623-32.